

# Composite Bi-2212/Ag superconductors grown by laser travelling floating zone at low rates

J.C. Diez<sup>1\*</sup>, A. Sotelo<sup>1</sup>, Sh. Rasekh<sup>1</sup>, H. Amaveda<sup>1</sup>, M. A. Torres<sup>1</sup>, P. Bosque<sup>2</sup>, C. Chocarro<sup>3</sup>, M.A. Madre<sup>1</sup>

<sup>1</sup>ICMA (CSIC-Universidad de Zaragoza). María de Luna, 3. 50018-Zaragoza. Spain.

<sup>2</sup> Centro Universitario de la Defensa, Academia General Militar, Ctra Huesca s/n, 50090-Zaragoza (Spain).

<sup>3</sup>Universidad de Lleida, Dpto. de Producción Vegetal y Ciencia Forestal, C/ Rovira Roure 191, E-25198, Lleida (Spain)

\* Corresponding author: J. C. Diez, [monux@unizar.es](mailto:monux@unizar.es); Tel: +34 976762526; Fax: +34 976761957

## ABSTRACT

Well textured  $\text{Bi}_{2.02}\text{Sr}_{2.02}\text{Ca}_{0.98}\text{Cu}_{1.99}\text{O}_x$  /2.9 wt.% Ag composite samples have been grown by the laser floating zone at very low rates (1, 3, and 5 mm/h). The as grown samples present superconducting behavior, as a result of being composed by long and well textured Bi-2212 grains as major phase. After annealing the samples do not increase dramatically their  $J_C$ . This effect has been associated with the presence of long cracks between superconducting grains along their  $ab$  planes. Even after annealing, the cracks have not been totally removed and, as consequence, the critical current of the samples after the thermal treatment has only been improved in around 50%, compared with the as grown samples.

Keywords: Bi-2212, Ag, Directional growth, Critical current, Composite

## 1. INTRODUCTION

The development of commercial applications based on high temperature superconductors requires the use of texturing techniques in order to obtain bulk materials with high critical current density ( $J_C$ ) values [1]. These techniques must be reliable enough in order to assure the high  $J_C$  in long-lengths [2]. Although  $(\text{Bi},\text{Pb})_2\text{Sr}_2\text{Ca}_2\text{Cu}_3\text{O}_{10+\delta}$  (Bi-2223) superconductors have a high critical temperature,  $T_C$ , of  $\sim 110$  K,  $\text{Bi}_2\text{Sr}_2\text{CaCu}_2\text{O}_{8+\delta}$  (Bi-2212) superconductors, with lower  $T_C \sim 90$ -95 K,

requires less complex reaction and texturing processes. Therefore Bi-2212 superconductors have demonstrated that they are suitable for many applications when properly processed, as for example by the laser floating zone (LFZ), where well textured bulk materials are obtained [3,4]. Recently, this technique has also been successfully used with other plate-like grain ceramic materials [5,6].

The superconducting materials textured by the LFZ technique have very well aligned crystals, with their *c*-axis perpendicular to the current flow direction and strong grain boundaries. Bulk Bi-2212 LFZ textured materials show  $J_C$  values higher than 5000 A/cm<sup>2</sup> for ~1mm diameter rods [6]. This method can be improved by an electrical current crossing the melt, called electrical assisted laser floating zone (EALFZ), which is able to obtain Bi-2212 samples with improved texture [7] when compared with the classical LFZ technique. In any case, the interesting transport properties obtained in these bulk Bi-2212 textured materials allow developing practical applications, as current leads [8] or fault current limiters [9]. One of the main advantages of this method is that the materials can be rapidly grown due to the large thermal gradient at the solid-liquid interface [10,11]. A second additional advantage is the absence of crucible, avoiding external contamination of textured samples during the processing. However, the poor mechanical characteristics of this kind of materials [12,13] due to their ceramic nature, imposes some limitations for practical applications. Some attempts to improve their mechanical behavior have been performed by means of Ag addition on BSCCO compounds [9,14] and other plate like grain ceramics [15]. The aim of this work is to study well textured Bi-2212/Ag composites, with Ag content fixed in ~3 wt. %, when the texturing process is performed by means of the LFZ technique at very low rates ( $\leq$ 5 mm/h), in order to stabilize the solidification front. The changes on the microstructure are related with the superconducting properties of the samples.

## 2. EXPERIMENTAL

Green ceramic cylindrical precursors, ~120 mm long and ~3 mm diameter, have been prepared from commercial  $\text{Bi}_{2.02}\text{Sr}_{2.02}\text{Ca}_{0.98}\text{Cu}_{1.99}\text{O}_x$  /2.9 wt.% Ag composite powder precursors (Nexans SuperConductors GmbH) by cold isostatic pressing with an applied pressure of 200 MPa during 1 minute. The obtained green cylinders were subsequently used as feed in a directional solidification process performed in a LFZ installation described elsewhere [16]. These bars have been processed using a continuous power Nd:YAG laser ( $\lambda = 1064$  nm), under air, at growth rates of 1, 3, and 5 mm/h. In the

process, the seed has been rotated clockwise at 3 rpm in order to maintain the cylindrical geometry while the feed has been rotated anticlockwise at 15 rpm to homogenize the molten zone. Finally, after the growth process, the textured bars, about ~150 mm length and ~2 mm diameter, have shown to be very homogeneous dimensionally. These rods were then cut into several pieces with the adequate dimensions (~35 mm long) for their electrical characterization both, as grown and after annealing. This thermal process was performed under air, and consisted in two steps: 60 h at 860 °C to produce the maximum amount of Bi-2212 phase, followed by 12 h at 800 °C to adjust the oxygen content in the superconducting phase and, finally, quenched in air to room temperature. Moreover, four silver contacts were painted on these samples, two of about 5 mm at both ends of the bars for the current injection and two small ones in the center of the bar, with ~1 cm between them, for the voltage measurements. Morphological and microstructural characterization, before and after annealing, was made on polished longitudinal cross-sections of the samples in a field emission scanning electron microscope (FESEM, Zeiss Merlin) equipped with an energy dispersive spectroscopy (EDX) system. Powder X-ray diffraction (XRD) patterns have also been recorded, with  $2\theta$  ranging between 5 and 40 degrees, in order to identify the different phases (Rigaku D/max-B X-ray powder diffractometer working with Cu K $\alpha$  radiation).

Electrical measurements were performed by the conventional four-point probe configuration in both, as grown and annealed samples. Resistivity as a function of temperature, from 77 to 300 K, was measured using a dc current of 1 mA. Critical current density ( $J_C$ ) values were determined at 77 K, from the I-V curves, using the 1  $\mu$ V/cm standard criterion.

### 3. RESULTS AND DISCUSSION

Fig.1 shows representative SEM images of as-grown samples grown at different rates. Although the heat treatment has not been performed in these samples, the major phase (grey contrast matrix) corresponds to the superconducting Bi-2212 one. It is also possible to find some Bi-free secondary phases (dark contrast, indicated by #1), which have been identified by EDX as Sr-Ca-Cu-O ones. The amount of these secondary phases is increasing when the growth rate is raised, due to the destabilization of the solidification front, as it can be observed when comparing Fig. 1a (1mm/h) and Fig. 1b

(3 mm/h). In addition, it is also possible to find some scattered small CaO crystals in these as-grown samples, probably associated with local instabilities of the solidification front. Although it cannot be clearly seen on these micrographs, small intergrowths of Bi-2212 and Bi-2201 can be found close to the Bi-free secondary phases. In any case, as a result of the low growth rates used in this work, the major phase is always the Bi-2212 one, that it is appearing as long grains (hundreds of microns), with their *ab* planes parallel to the growth direction. However, as a result of the strong thermal shock produced in these big size grains during the solidification, long cracks along the *ab* planes (marked as #2 in Fig. 1) appear. On the other hand, metallic Ag (light grey contrast, indicated by #3) is finely distributed inside the superconducting grains (see Fig. 1d). Furthermore, it can be also been found as elongated grains filling the gaps between superconducting grains (see Fig. 1c). When the samples are annealed, not noticeable changes have been detected. Cracks are still easily found between Bi-2212 grains and only a small decrease in the amount of secondary phases is observed. This last feature is confirmed by the powder XRD patterns performed in the as-grown and annealed samples. In Fig. 2 representative patterns for the as-grown and annealed samples prepared at 3 mm/h, are presented. As it can be clearly seen in the figure, only small differences appear between both XRD patterns. At first sight, it is possible to see that the Bi-2212 is the major phase (peaks indicated by  $\nabla$  in the figure [17]). On the other hand the identification of the main peak of Bi-2201 phase [17] at  $\sim 29.7^\circ$  (marked with  $\blacklozenge$ ) with very small intensity, clearly indicates the low content of this phase. This is in agreement with the microstructural features as discussed previously. Moreover, the peak appearing at around  $38.2^\circ$  corresponds to the (111) diffraction plane of metallic Ag (marked as #). Finally, the symbol \* identifies the Bi-free secondary phase [18] which is decreasing after the thermal treatment. The main differences found in these patterns are due to the preferential orientation of the grains, as can be deduced from the variation observed in the relative intensities of the  $(00l)$  peaks. This effect can be associated to the samples preparation which can induce different preferential grain orientations in the powdered samples.

The electrical characteristics of the samples, both as-grown and annealed are displayed in Table I. As it is reflected in these data, all the samples show a similar  $T_C$ , indicating that as-grown and annealed samples possess, approximately, the same oxygen content in the Bi-2212 grains, indicating that the oxygenation thermal treatment is unnecessary in samples grown at these low rates. In all the cases the samples display a metallic

behavior at temperatures well above the transition one, as it is expected for Bi-2212 superconductors.

When considering the critical current intensities, it can be observed that higher growth rates produce higher  $I_C$ . This effect is related with the bigger grain sizes obtained with the lower growth speeds. These larger grain sizes promote the formation of higher thermal stresses and, as a consequence, the formation of bigger cracks. Moreover, after the thermal treatment, a slight raise in  $I_C$  can be observed which is clearly indicating that the annealing process has been not able to totally remove the cracks. In spite of the presence of these remaining cracks, an  $I_C$  raise of about 50% has been reached in all the cases. As can be regarded in Table I and in Fig. 3,  $J_C$  is increasing with the growth speed. Moreover, annealing process lead to higher  $J_C$  values compared with the as grown ones, but keeping the same trend (higher growth speed led to higher  $J_C$  values), confirming the previous discussions about  $I_C$  evolution. Finally, the obtained  $J_C$  in these samples grown at low rates, even after the thermal treatments, are far lower than the obtained in previously reported data on Bi-2212/Ag composites grown at higher speeds [14] which avoid cracks formation.

#### 4. CONCLUSIONS

$\text{Bi}_{2.02}\text{Sr}_{2.02}\text{Ca}_{0.98}\text{Cu}_{1.99}\text{O}_x$  /2.9 wt.% Ag ceramics were successfully grown through a LFZ process at very low rates (1, 3, and 5 mm/h). After the growth processes all the samples are mainly composed by big and well aligned Bi-2212 grains. The Ag has been found as small precipitates inside the grains and, in some cases, as elongated particles between the Bi-2212 grains. As a result of the cracks formed between the superconducting grains,  $J_C$  values are between 1000 (1 mm/h) and 1500 (5 mm/h) A/cm<sup>2</sup>. After annealing process, cracks were only partially removed, leading to an increase of about 50% on the  $J_C$ . In any case, these low growth rates can be used to obtain single grains in an easy and quick manner.

#### ACKNOWLEDGEMENTS

The authors acknowledge financial support from the Gobierno de Aragón (Consolidated Research Groups T12 and T87) and MINECO-FEDER (MAT2013-46505-C3-1-R). M. A. Madre acknowledges the MINECO-FEDER (Project MAT2011-22719) for funding. The technical contribution of C. Estepa, and C. Gallego are also acknowledged. Sh. Rasekh acknowledges a JAE-PreDoc 2010 grant from CSIC. Authors would like to

acknowledge the use of Servicio General de Apoyo a la Investigación-SAI, Universidad de Zaragoza.

## REFERENCES

- [1] Chen, M., Donzel, L., Lakner, M., Paul, W.: *J. Eur. Ceram. Soc.* 24, 1815-1822 (2004).
- [2] Larbalestier, D.C., Jiang, J., Trociewitz, U.P., Katemani, F. Scheuerlein, C., Dalban-Canassy, M., Matras, M., Chen, P., Craig, N.C., Lee, P.J., Hellstrom, E.E.: *Natur. Mat.* (2014) DOI: 10.1038/NMT3887.
- [3] Mora, M., Diez, J.C., Lopez-Gascon, C.I., Martinez, E., de la Fuente, G.F.: *IEEE Trans. Appl. Supercond.* 13, 3188-3191 (2003).
- [4] Carrasco, M. F., Costa, F. M., Silva, R. F., Gimeno, F., Sotelo, A., Mora, M., Diez, J. C., Angurel, L. A.: *Physica C* 415, 163-171 (2004).
- [5] Constantinescu, G., Rasekh, Sh., Torresa, M.A., Madre, M.A., Diez, J. C., Sotelo, A.: *Scr. Mat.* 68, 75-78 (2013).
- [6] Angurel, L.A., Diez, J.C., de la Fuente, G.F., Gimeno, F., Lera, F. Lopez-Gascon, C.I., Martinez, E., Mora, M., Navarro, R. Sotelo, A., Andres, N., Recuero, S., Arroyo, M.P.: *Phys. Status Solidi A-Appl. Mat.* 203, 2931-2937 (2006).
- [7] Costa, F.M., Rasekh, Sh., Ferreira, N.M., Sotelo, A., Diez, J.C., Madre, M.A.: *J. Supercond. Nov. Magn.* 26, 943-946 (2013).
- [8] Garcia-Tabares, L., Calero, J., Abramian, P., Toral, F., Angurel, L.A., Diez, J.C., Natividad, E., Iturbe, R., Etxeandia, J.: *IEEE Trans. Appl. Supercond.* 11, 2543-2546 (2001).
- [9] Sotelo, A., Madre, M.A., Rasekh, Sh. Diez, J.C., Angurel, L.A.: *Adv. Appl. Ceram.* 108, 285-289 (2009).
- [10] Feigelson, R.S., Gazit, D. Fork, D.K., Geballe, T.H.: *Science* 240, 1642-1645 (1988).
- [11] Revcolevschi, A., Jegoudez, J.: *Prog. Mater. Sci.* 42, 321-339 (1997).
- [12] Diez, J.C., Sotelo, A., Mora, M., Amaveda, H., Madre, M.A.: *J. Eur. Ceram. Soc.* 27, 3963 (2007).
- [13] Diez, J.C., Constantinescu, G., Rasekh, S., Estepa, L.C., Madre, M.A., Sotelo, A.: *J. Supercond. Nov. Magn.* 26, 895-900 (2013).
- [14] Mora, M., Sotelo, A., Amaveda, H., Madre, M.A., Diez, J.C., Angurel, L.A., de la Fuente, G.F.: *Bol. Soc. Esp. Ceram. Vidr.* 44, 199-203 (2005).
- [15] Sotelo, A., Torres, M.A., Constantinescu, G., Rasekh, Sh., Diez, J.C., Madre, M.A.: *J. Eur. Ceram. Soc.* 32, 3745-3751 (2012).

- [16] Sotelo, A., Rasekh, Sh., Madre, M.A., Diez, J.C.: *J. Supercond. Nov. Magn.* 24, 19 (2011).
- [17] Torardi, C. C.: Structural details of the high  $T_C$  copper based superconductors. In: Vanderah, T. A. (ed.) *Chemistry of superconductor materials-Preparation, chemistry, characterization and theory*, pp: 501-540. Noyes Publications, Park Ridge-New Jersey (1992).
- [18] Sotelo, A., Majewski, P., Park, H.-S., Aldinger, F.: *Physica C* 272, 115-124 (1996).

**Table I.** Superconducting properties ( $T_C$ ,  $I_C$  and,  $J_C$ ) for the as grown and annealed samples as a function of the LFZ growth rate. The diameter of the samples is also displayed.

<b>Growth rate</b>	<b>As grown</b>			<b>After annealing</b>		
	<b>1 mm/h</b>	<b>3 mm/h</b>	<b>5 mm/h</b>	<b>1 mm/h</b>	<b>3 mm/h</b>	<b>5 mm/h</b>
$T_C$ (K)	~90.5	~90.5	~90.5	~90.5	~90.5	~90.5
$I_C$ (A)	32.3	36.5	51	49.5	53.6	74
$d$ (mm)	2.04	2.04	2.04	2.00	2.00	2.00
$J_C$ (A/cm <sup>2</sup> )	988	1116	1651	1576	1707	2357

## Figure captions

**Figure 1.** Representative SEM micrographs performed on transversal (a, b, and d) and longitudinal (c) polished samples grown at: (a) and (c) 1 mm/h, (b) and (d) 3 mm/h. Grey matrix is Bi-2212 phase. #1 indicates Bi-free secondary phases, #2 cracks, #3 metallic Ag

**Figure 2.** Representative powder XRD patterns of the Bi-2212/3 wt.%Ag obtained at 3 mm/h on as as-grown (a) and annealed samples (b).  $\nabla$  indicates the Bi-2212 peaks,  $\blacklozenge$  Bi-2201, \* Bi-free secondary phases, and # metallic Ag.

**Figure 3.**  $J_C$  values as a function of the growth rate for both, as grown samples and annealed ones.

**Figure 1**

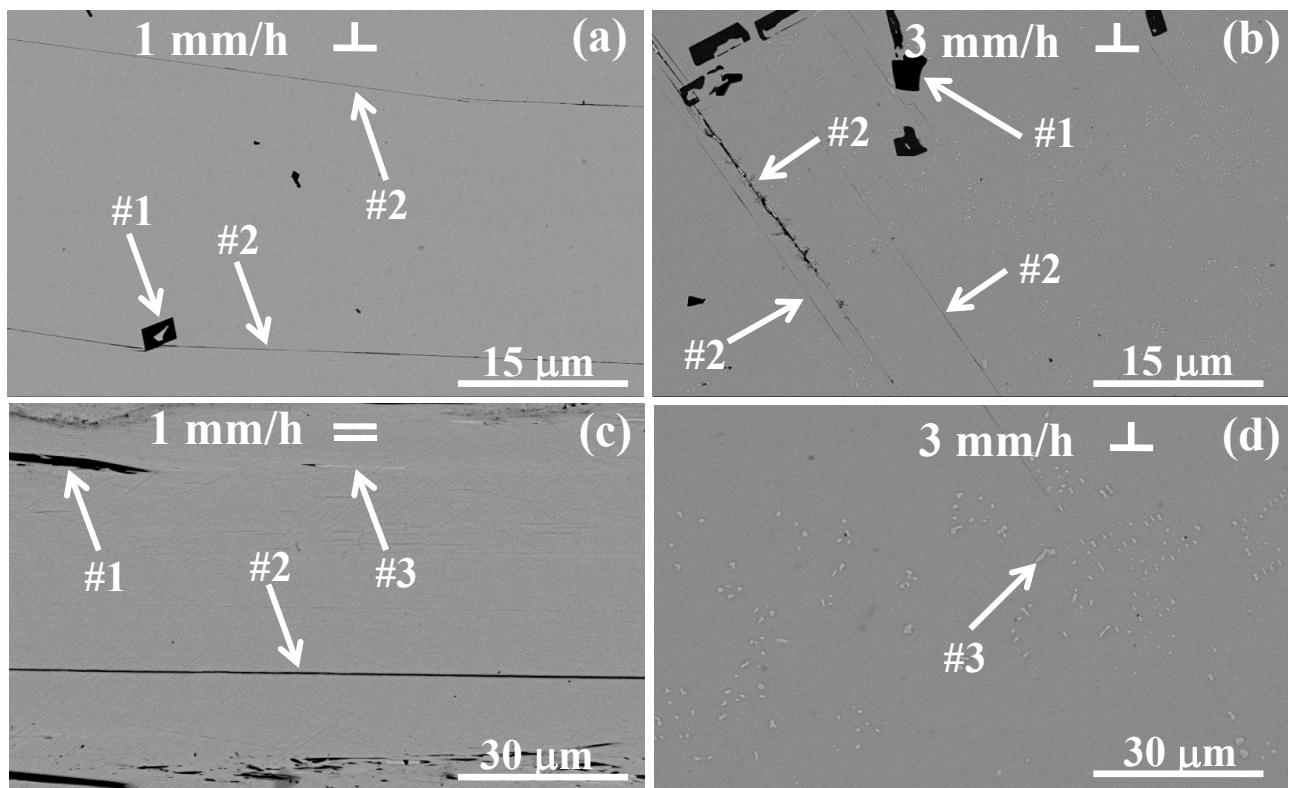
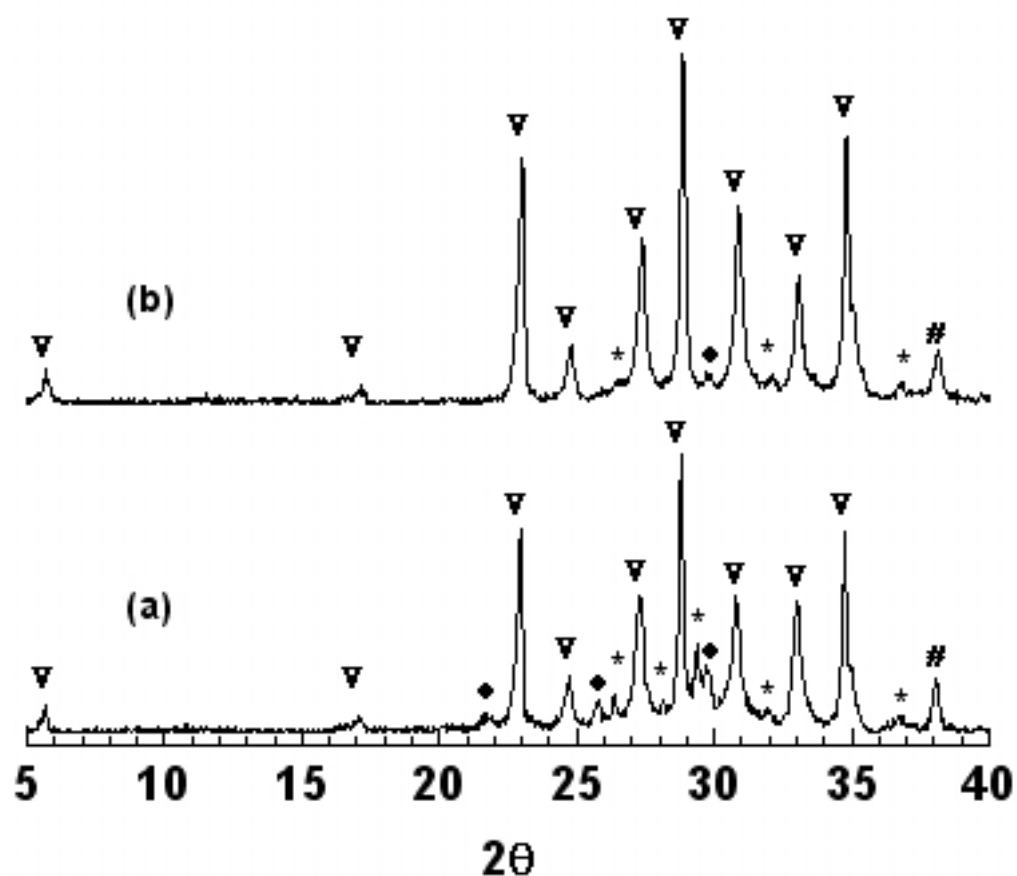


Figure 2



**Figure 3**

